

Three-Dimensional Printing of Double-Network Hydrogels: Recent Progress, Challenges, and Future Outlook

Puskal Kunwar, Mark James Ransbottom, and Pranav Soman

Abstract

Hydrogels are widely used materials due to their biocompatibility, their ability to mimic the hydrated and porous extracellular microenvironment, as well as their ability to tune both mechanical and biochemical properties. However, most hydrogels lack mechanical toughness, and shaping them into complicated three-dimensional (3D) structures remains challenging. In the past decade, tough and stretchable double-network hydrogels (DN gels) were developed for tissue engineering, soft robotics, and applications that require a combination of high-energy dissipation and large deformations. Although DN gels were processed into simple shapes by using conventional casting and molding methods, new 3D printing methods have enabled the shaping of DN gels into structurally complex 3D geometries. This review will describe the state-of-art technologies for shaping tough and stretchable DN gels into custom geometries by using conventional molding and casting, extrusion, and optics-based 3D printing, as well as the key challenges and future outlook in this field.

Keywords: double-network hydrogel, 3D printing, DLP printing, molding and casting, extrusion printing

Introduction

HYDROGELS ARE SOFT, hydrated materials with three-dimensional (3D) crosslinked networks. They have been used in many biomedical applications such as tissue engineering, drug-delivery systems, and super absorbents.^{1–4} These networks of hydrophilic polymers can hold large amounts of water owing to their physical, chemical, or biochemical crosslinking of individual polymer chains.^{2,5,6} Physical crosslinking occurs in response to changes in environmental conditions such as pH, temperature, or ionic concentration, whereas chemical crosslinking introduces mechanical integrity and degradation resistance due to covalent bonding. Further, biochemical crosslinking agents such as enzymes or amino acids can also induce polymerization in hydrogels. However, hydrogels are, in general, mechanically weak with poor toughness, limited in deformation and recoverability because of their structure heterogeneity and/or lack of efficient energy-dissipation mechanism. This has restricted the extensive use of hydrogels in science and industry.^{7,8}

In recent years, significant efforts have been made to synthesize mechanically strong and flexible hydrogels such as interpenetrating polymer network (IPN) gels,^{9,10} nanocomposite hydrogels,¹¹ slide-ring hydrogels,¹² macromolecular

microsphere composite (MMC) hydrogels,¹³ triblock copolymers hydrogels, and¹⁴ tetra-PEG (polyethylene glycol) gels.¹⁵ Of the aforementioned list, IPN gels are mechanically strong hydrogel systems that consist of two or more hydrogel networks that are at least partially entangled. IPN gels with two networks, typically one ionic and the other covalent, are called Double-Network Hydrogels (DN gels) (Fig. 1).^{9,16–18} In general, one of the hydrogel networks in DN gels provides material toughness, whereas the other network prevents macroscopic crack propagation through energy dissipation. Thus, DN gels exhibit significantly better mechanical properties than either of the parent gels. The DN gels consist of 65–95 wt % water, yet they exhibit fracture toughness that is comparable to many elastomeric materials and connective tissues such as ligaments.^{9,10,16–18}

One of the common strategies of synthesizing DN gels is to first prepare a template of a crosslinked, negatively charged hydrogel, into which a large amount of neutral hydrogel can perfuse into and undergo crosslinking.^{9,19} Using this technique, poly(2-acrylamide-2-methylpropane sulfonic acid) PAMPS/polyacrylamide (PAAm) DN gel was synthesized back in 2003. Here, a negatively charged PAMPS hydrogel was used as the first network where polyacrylamide perfused inside the PAMPs network and formed DN gels. This DN gel

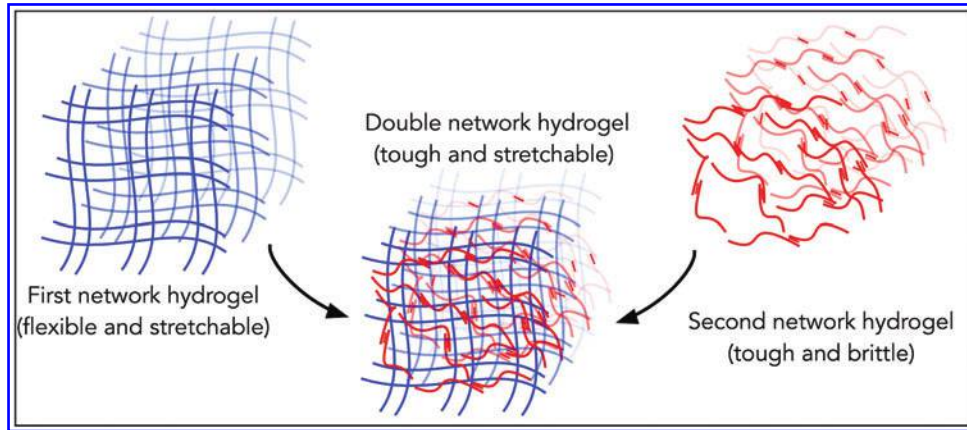


FIG. 1. Schematic showing the basic structure of DN gels. DN gels, double-network hydrogels. Color images are available online.

had the fracture toughness of 10^2 – 10^3 J · m⁻², fracture tensile stress of 1–10 MPa, and fracture tensile strain of 1000–2000%.²⁰ Since 2003, different strategies have been used to synthesize DN gels with unique mechanical properties. Several synthesis routes such as a two-step polymerization method,²⁰ molecular stent method,^{21,22} freeze-drying method,²² one pot synthesis method,^{23,24} and 3D printing^{9,25–27} have been used to synthesize different DN gels networks such as PAAM/alginate,^{28,29} PAAM/ κ -carageneen,^{26,30} polyurethane (HTPU) hydrogel/PAAM,³¹ PEG/agarose,³² polyvinyl alcohol (PVA)/PAAM DN gel,³³ agar/PAAM DN,^{34,35} Li₂SO₄-containing agarose/polyacrylamide double-network (Li-AG/PAM DN),³⁶ and alginate/gelatin.³⁷ Further, there are reports of DN gels that are biocompatible and support high cell viability, proliferation, and cell functionality.^{38–42}

Synthesis of these DN gels has resulted into many applications in different fields.^{9,16,19} Tissue engineering and repair of cartilage tissue is considered one of the most prominent applications of DN gels. Cartilage is a connective tissue found in joints, on the ends of the ribs, between the vertebrae,

etc. and is composed of specialized cells called chondrocytes. Cartilage is avascular, and it is difficult to repair compared with the other tissues of the human body. The DN gels have been shown to have promise in the growth of chondrocytes and repair of existing cartilage.^{38,42,43} Other applications include fibroblast cell growth,⁴⁴ endothelial cell adhesion,⁴⁵ drug delivery and reservoirs,^{46,47} antifouling materials,^{48,49} sensors, actuators,^{26,50} soft optics⁵¹ etc. Detailed information about the DN gels is covered in review articles on this topic from the leading researchers in the field.^{9,16,19,50}

The most common method used to fabricate DN gels is molding and casting. (Fig. 2).⁵² In this method, prepolymer solution is cast into a mold followed by polymerization via a range of crosslinking agents such as light, chemicals, or heat. Although this method has several advantages such as simplicity, high throughput, and low cost,⁶ and has already been used in fields of tissue engineering, flexible optics, and soft robotics, printing of complex DN gels at high resolution remains a challenge with this method. Hence, newer additive fabrication techniques such as in extrusion-based 3D printing

Casting and molding based fabrication approach	Extrusion based fabrication approach	Optics based fabrication approach
<p><u>DN gels:</u></p> <ul style="list-style-type: none"> -PAMPS/PVA -PAMPS/PAAM -Alginate/PAAM -Agar/PAAM -Agarose/PEG -PVA/PAAM 	<p><u>DN gels:</u></p> <ul style="list-style-type: none"> -Alginate/PAAM -Alginate/PEGDA -Agar/alginate -norbornene HA/HA-hydrazone -AMPS/PAAM -k-carrageenan/PAAM -k-carrageenan/GelMA 	<p><u>DN gels:</u></p> <ul style="list-style-type: none"> -Alginate/metharylated-alginate -PAAM/PEGDA -Alginate/PAAM
<p><u>Applications</u></p> <p>artificial meniscus, scaffolds for cell viability and proliferation studies, piezoresistive sensor</p>	<p><u>Applications</u></p> <p>artificial meniscus, bioprinting applications, scaffolds for cell viability and proliferation studies, strain sensors</p>	<p><u>Applications</u></p> <p>scaffolds for cell viability and proliferation studies, flexible optics, flexible and stretchable electronics</p>

FIG. 2. Overview of different fabrication techniques for printing different DN gels' structures. Color images are available online.

and high-resolution optical projection lithography (OPL) are receiving growing interest for printing 3D complex DN gels structures.^{26,51,53,54}

This review summarizes the recent work on the 3D printing of high-strength and elastic DN gels based on three methods, (1) casting and molding, (2) extrusion-based 3D printing, and (3) optics-based 3D printing. This review also explores the challenges faced by the field and discusses its future outlook in the context of improving 3D printing complexity/resolution along with potential applications.

Casting and Molding of DN Gel Structures

Casting and molding is the most widely technique for the fabrication of DN gels structures. This method involves the pouring of hydrogel precursor solution into a hollow cavity with desired shape, followed by crosslinking mediated by light, chemicals, or thermal stimulus. The crosslinked hydrogels then adopt the shape of the mold (Fig. 3A). This robust method has been used to fabricate simple, planar, and disk-shaped two-dimensional (2D) structures in DN gels.^{55–57}

Fabrication of DN gels into well-defined and mechanically robust structures is crucial for several applications. For

example, artificial tissue such as cartilage and tendon requires high mechanical performances under stress. Earlier, DN gels synthesized by the classical and molecular stent methods were difficult to carve into a complex shape as the first network that determined the shape of the DN gel was unable to preserve its mechanical integrity on swelling.^{9,55} Back in 2010, Gong and coworkers discovered a new solution and synthesized free-shape DN gels structure by using a PAMPS/PVA interpenetrating network. They physically crosslinked PVA into a skeleton by using internal molds. These cross-linked structures were relatively tough and flexible and could form a relatively complex shape. Next, they polymerized a PAMPS network in the crosslinked PVA gels, forming the PVA/PAMPS network. Finally, they synthesized a PAAm network in the presence of PVA/PAMPS gels that resulted in triple-network gels called PVA-DN gels. Using this technique, they demonstrated the fabrication of the complex structures such as birds, fish, and Chinese knots (Fig. 3B). These structures exhibited mechanical properties similar to those of conventional DN gels.⁵⁵

The next year, Yasuda and his co-workers also showed the fabrication of a PAMPS-based DN gel structure. First, they prepared dry microparticles of PAMPS gel with a diameter of

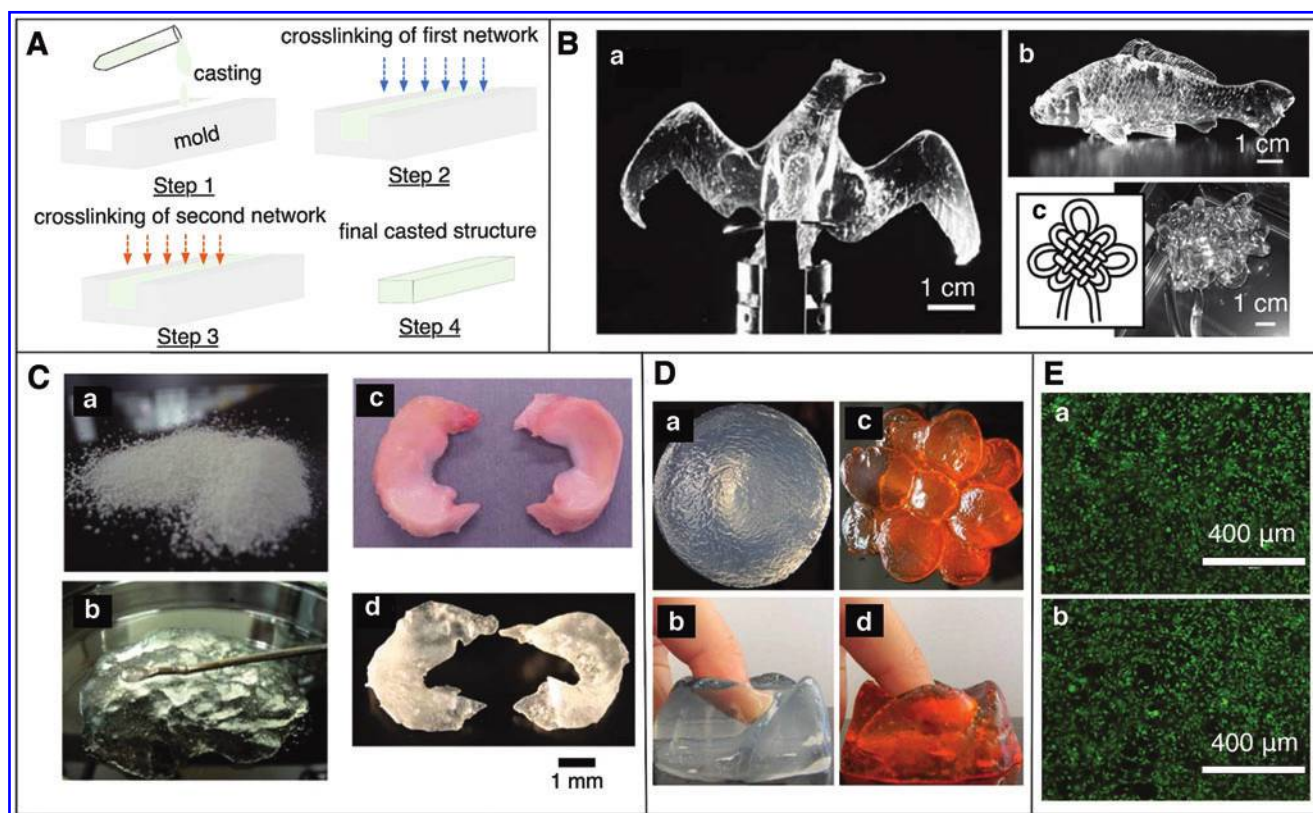


FIG. 3. (A) Schematic cartoon showing the casting and molding-based fabrication of DN gel structures. (B) Casting and molding approach of printing PVA-DN gels. Fabrication of complex structures such as (B.a) bird (B.b) fish and (B.c) Chinese knots.⁵⁵ (C) Casting and molding of printing PAMPS/AAM gel (C.a) dried powder of PAMPS particle (C.b) PAMPS particles in AAm solution before crosslinking (C.c) real rabbit meniscus (C.d) Cast meniscus from the PAMPS/AAM DN gels.⁵⁶ (D) Casting and molding of Alginate/PAAm gel into (D.a) ball-shaped structure (D.b) ball-shaped structure compressed with finger (D.c) flower-shaped structure (D.d) flower-shaped structure compressed with finger.⁵⁷ (E) Cell viability studies of mouse mesenchymal stem cells cultured in Alginate/PAAm gel for 3 days. Live–dead images of the cells cultured on (E.a) control sample (no gel), (E.b) DN gels structure. *Green color* represents live cell, whereas *red color* represents dead cells.²⁹ AAm, acrylamide; PAAm, polyacrylamide; PAMPS, poly(2-acrylamide-2-methylpropane sulfonic acid); PVA, polyvinyl alcohol. Color images are available online.

several tens of micrometers, and then soaked them in acrylamide (AAM) solution, forming a paste-like solution. They polymerized the paste-like solution, forming a DN gel and called it a P-DN gel. They fabricated an artificial meniscus, which resembled a rabbit meniscus (Fig. 3C) by using the P-DN gels. It is worth knowing that a meniscus is a C-shaped fibrous cartilage found between the surface of joints and acts as a cushion between the bones. The P-DN exhibited high strength, however the structures were limited in printing resolution.⁵⁶

In a pioneering study in 2012, Suo and colleagues reported the synthesis of DN gel structures from two polymers forming ionically and covalently crosslinked networks. They used PAAm as the first polymer and alginate as the second. The photo-initiator ammonium persulfate (APS) and crosslinker N,N, methylenebisacrylamide (MBAA) were added to photocrosslink PAAm, whereas calcium sulfate was added to ionically crosslink alginate. The prepolymer solution was poured into a glass mold with a dimension of $75 \times 150 \times 3 \text{ mm}^3$, and the solution was cured by using ultraviolet (UV) light. These structures exhibited extraordinary mechanical properties; they could be stretched beyond 20 times their initial length and were notch insensitive. They had fracture energies of $9000 \text{ J} \cdot \text{m}^{-2}$, which is one order of magnitude higher than that of the cartilage as compared with conventional hydrogels that are brittle and exhibit fracture energies of about $10 \text{ J} \cdot \text{m}^{-2}$.

The enhanced mechanical properties of the Alginate/PAAm DN gels were due to the combined effect of two mechanisms. The first mechanism was the energy dissipation on stretching provided by the ionically crosslinked alginate, whereas the second mechanism was the covalent crosslinked long PAAm polymer chain, which allowed for crack bridging that maintained mechanical integrity once the ionic crosslinks were broken. Further, on unloading of the large deformation, the covalent network returned to the initial states and the ionic bond healed by re-zipping. This work, which resulted in DN gels that were highly elastic, tough, and exhibit recoverability of stiffness and toughness, does not highlight the 3D fabrication of the DN gels into a complex structure but to a simple planar structure.²⁸ This material composition has been investigated for printing complex shapes and biocompatibility studies by many other research groups. For instance, Rao and colleagues reported synthesis and fabrication DN gel structures using an IPN of PAAm/sodium alginate in the presence of a crosslinker, MBAA, a UV initiator, APS, and calcium chloride. Using the same material system, they were able to mold relatively complex structures such as a ball and differently shaped flowers (Fig. 3D).⁵⁷

Similarly, Mooney and coworkers used the same material system and studied the biocompatibility and mechanical properties of the alginate/AAM gels under cell culture conditions. They reported a compressive strain of 90% with remarkably small loss of Young's Modulus and minimum swelling when the structures were soaked for 50 days in cell culture conditions. They fabricated a planar DN gel disk and examined the *in vitro* cell viability, metabolic activity, and proliferation of mouse mesenchymal stem cells. They found that, in general, these DN gel structures were not toxic, and cell proliferation and metabolic activities were only slightly reduced after continuous long exposure of cells to the structures (Fig. 3E). Further, they implanted the structure within subcutaneous tissue of rats for 8 weeks and performed histological studies, which suggested that the structures were non-immunogenic and non-inflammatory in nature.²⁹

In another study, Zheng and colleagues replaced alginate with agar and used the one-pot synthesis method to generate and fabricate highly mechanical and recoverable Agar/PAAm DN gels. Similar to earlier studies, light was used to covalently crosslink PAAm in the presence of crosslinker MBAA and photoinitiator Irgacure 2959. Agar biopolymer was used as the second polymer, as it exhibits thermoreversible sol-gel transition. This polymer forms solution when heated and gels on cooling. This transition is attributed to the coil-helix structural transition between high and low temperatures. Hence, the phase transition from a solution to gel was used to physically crosslink the second network of the DN gels (Fig. 4A). The as-synthesized Agar/PAAm exhibited both high toughness and strain. The authors reported that the structures showed maximum compression stress of 38 MPa, fracture strain of 98%, and elastic modulus of 123 kPa. The ultimate strain and tensile strength were around 2000% and 1.0 MPa, respectively. More importantly, they could be cast in the mold to fabricate 3D custom structures such as a teddy bear shaped structure with fine facial features. The bear was compressed and released; however, no remarkable change to the structure was observed. The fabricated structures could withstand deformation such as knotting, compression, and elongation without any observable damage (Fig. 4A).⁵⁸

Similarly, the casting and molding-based approach was used to shape PEG/agarose DN gels by using thermoreversible transition. Wu and colleagues prepared DN gels simply by mixing four-armed poly(ethylene glycol) amine (4 arm PEG-NH₂) agarose solution and four-armed poly(ethylene glycol) succinimidyl (4-arm-PEG-NHS) agarose solution into the phosphate buffer solution. This solution was put into molds; then, it was cooled down to obtain structures with a predefined shape and size. Structures such as clovers, letters "ICCAS," snowflakes, and hearts were successfully fabricated by using this approach.

The PEG/agarose DN gels showed an excellent compressive fracture strain of 98% and a compressive stress of 28.8 MPa, which was about 10 times higher than single-network tetra-PEG hydrogel metrics. The surface of these structures was biocompatible and was also favorable for cell growth, as the agarose improved the cell attachment ability of the PEG hydrogels that were otherwise not suitable for cell attachment due to their anti-fouling properties (Fig. 4B). Further, *in vivo* biocompatibility was also tested by implanting the DN gel structures subcutaneously into rats. The authors found that the structures showed an inflammatory response on day 3; however, the response was negligible by day 28, indicating that the DN gel structures did not lead to persistent inflammation.⁴⁴

In 2018, Dong and his team synthesized conductive hydrogel by using AAM and PVA. The hydrogel prepolymer solution was prepared by dissolving the PVA powder in hot water, which was followed by the addition of AAM monomer chemical crosslinker MBAA and oxidizer, APS. The conductivity and reaction rate of the solution was enhanced by adding potassium chloride (KCl) and N, N, N', N' tetramethylethylenediamine (TEMED). The prepolymer solution was exposed to UV for 120 min. The DN gels were formed through a sol-gel process that involves photo-polymerization of AAM and a physically crosslinked PVA network. Using a petri dish mold, they fabricated transparent planar disks, which were biocompatible and they exhibited high strain and

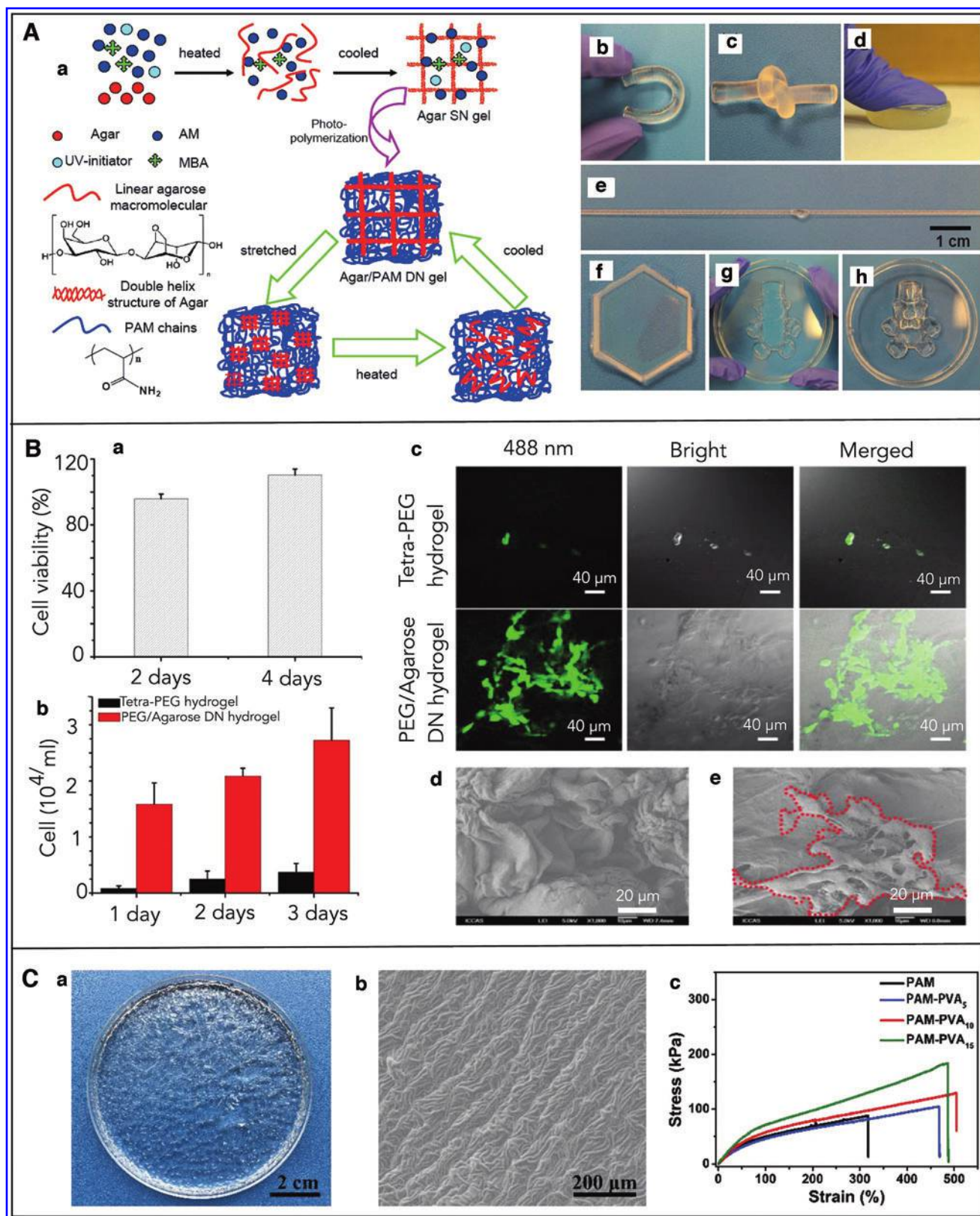


FIG. 4. (A) Casting and molding-based fabrication of Agar/PAAm DN gels. (A.a) Cartoon showing the synthesis procedure. Extraordinary mechanical properties of the DN gels' structure (A.b) bending; (A.c) knotting; (A.d) compression; (A.e) stretching; (A.f) hexagon; (A.g) teddy bear gel under compression; and (A.h) teddy bear gel after release.⁵⁸ (B) Casting and molding-based fabrication of PEG/agarose DN gels. (B.a) Cell viability of 3T3 fibroblast cells after incubation for 1 and 3 days on PEG/agarose substrate. (B.b) Number of 3T3 fibroblasts on tetra-PEG hydrogel and PEG/agarose DN gels after seeding them for 1, 2, and 3 days. (B.c) Confocal, bright-field, and merged images of fibroblast mouse cells cultured on the surface of tetra-PEG and PEG/agarose DN gels for 72 h. (B.d) SEM image of tetra-PEG hydrogel. (B.e) SEM image of PEG/agarose DN gels with fibroblast mouse cells (incubation period of 73 h).⁴⁴ (C) Casting and molding-based fabrication of PVA/PAAm DN gels: (C.a) large area DN gel disk, (C.b) SEM image showing the ridge pattern in the DN gels structure, (C.c) stress-strain curves of the DN gels with varying concentration of PVA (5, 10, and 15 mg mL⁻¹).⁵⁹ PEG, polyethylene glycol; SEM, scanning electron microscope. Color images are available online.

toughness. Interestingly, this DN gel structure's surface displayed uniform micropatterns with numerous 3D protruding microchannels, which resembled spinosum microstructures of the human epicuticle (Fig. 4C). This microstructure along with interconnected ridges increased the contact surface area and sensitivity of the piezo-resistive hydrogel-based sensor, which showed a fast response when compared with human skin.⁵⁹

Extrusion Based 3D Printing of DN Gels

Extrusion printing is an additive manufacturing method that is capable of fabricating complex 3D structures by dispensing the material out of a nozzle. The extruded material is deposited layer by layer onto a programmable stage, thereby creating 3D structures. The first layer is at least partially polymerized before the second layer is deposited.⁶⁰ Based on a computer aided design (CAD) file, this method can 3D print polymers, hydrogels with and without cells into structures with complex and reproducible geometries with a resolution of a few hundred micrometers (Fig. 5A).^{61,62} In the past decade, this technique of fabrication was used to print 3D structures by using DN hydrogels that are highly stretchable, mechanically tough, and mostly biocompatible.^{27,53,63}

In 2013, Spinks and colleagues demonstrated the extrusion printing of DN gels by using AAm/alginate ink. Calcium chloride solution was used as alginate crosslinker, and ethylene glycol was added to the ink as a co-solvent. The photocrosslinking of the AAm was aided by photo-initiator α -keto glutaric acid and crosslinker MBAA. A bioplotter extrusion system (KIMM SPS1000; Korea Institute of Machinery and Material) with a gauge extrusion nozzle 0.337 mm in diameter combined with the UV-curing system was used to fabricate DN gel structures by using AAm/alginate inks. Before printing, viscosity was used as a metric to determine the suitability of the alginate-acrylamide gels with various concentrations. They found that alginate solutions with concentration below 2% w/v were not suitable for extrusion printing due to low viscosity, which resulted in an unwanted spreading of the extrudate. However, alginate concentrations more than 2% w/v were used to successfully print different structures, including dog-bones with a resolution of around 300 μm (Fig. 5B).

The as printed structures in AAm/alginate ink exhibited an ultimate strain of 300% when using a 2% alginate sample, whereas a maximum stress of 200 kPa was observed for 5% alginate structures. The corresponding failure stress (220 kPa) and failure strain (900%) were better for manually fabricated structures, because they were devoid of the structural flaws introduced into the hydrogel due to 3D printing. Dipping the structures in the water also had a detrimental effect on the mechanical properties of the structure; however, post-printing, immersion in calcium ions further increased the alginate crosslinking and thereby preserved the properties and overall dimensions of the printed structures.⁶³

Zhao and coworkers replaced AAm with PEG and printed biocompatible DN gel structures consisting of sodium alginate and poly(ethylene glycol) diacrylate (PEGDA). PEGDA undergoes covalent crosslinking, whereas alginate ionically crosslinks to form DN gels. They reported that optimized DN gels with 20 wt % PEG and 2.5 wt % alginate exhibit maximum fracture energy comparable to articular cartilage,

whereas the ultimate strain of the structure reaches 600%. Next, they demonstrated the printing of PEG/alginate DN gels into complicated 3D structures. However, they added Laponite, a nanoclay, to obtain the suitable viscosity for extrusion-based printing. They used a Fab@Home Model 3 extrusion printer for printing different structures such as a hollow cube, hemisphere, pyramid, twisted bundle, the shape of an ear, and a nose (Fig. 5C). Further, they printed the mesh structure by using human embryonic kidney laden DN gels along with nanoclay and studied the cell viability, which showed high cell viability of 95% over the course of 7 days of culture.⁶⁴

Similarly, Cong and colleagues used agar, alginate, and PAAm to print DN gel 3D structures (Fig. 5D). They reported that the agar-based DN gel more closely matched the characteristics of ink for printing precise 3D structures. Further, they added alginate to the solution, improving the viscosity of the prepolymer solution. However, increasing the alginate concentration had a detrimental effect on ultimate strain due to the higher crosslinking density produced by the physical entanglement of alginate. A Leapfrog Creator 3D printer was used to print the structure after replacing the heater and nozzle of the printer with a light weight syringe. They reported that the tensile strength of the alginate/agar DN gels was higher than that of agar/PAAm DN gels and comparable to that of natural cartilage. The authors also claimed that these DN gels can be used as cartilage substitutes and this method of printing could be useful for printing organs that require higher mechanical performances.²⁵

Burdick and coworkers also used shear-thinning and self-healing hydrogels for printing 3D structures out of DN gels. Due to the shear thinning properties, hydrogel can extrude by breaking physical crosslinks, which crosslink again by utilizing the intrinsic self-healing mechanism. This is followed by secondary crosslinking to form a robust structure. In this work, they modified hyaluronic acid (HA) with either hydrazide or aldehyde groups and mixed them together to form hydrogels with dynamic hydrazone bonds. These bonds possessed dynamic covalent chemistry, which gave them the properties of shear thinning and self-healing, which were needed for the extrusion-based printing. Next, they added norbornene-modified HA, a photocrosslinkable network, PETMA crosslinker, a tetrathiol, and the photoinitiator Irgacure 2959 to the modified HA hydrogels and printed DN gels structures with improved mechanical properties (Fig. 6A). They believed that this fabrication method could be used to fabricate complex biological scaffolds with spatial control of heterogeneity in the mechanics and the spatial location of biomolecules.²⁷

Stretchable and self-healing structures were also printed by using DN gels of the κ -carrageenan/PAAm network, thanks to thermo-reversible sol-gel transition of κ -carrageenan. κ -carrageenan is a biocompatible polysaccharide and undergoes ionic crosslinking. The prehydrogel solution consisted of the κ -carrageenan/AAm solution, potassium ion for ionic crosslinking of the carrageenan, crosslinker MBAA, and UV initiator for crosslinking AAm. A 3D bioprinter (BioFactory; regenHU Ltd.) was used to print the DN gel structures. Before printing structures, rheological properties of the material were studied. At high temperatures, κ -carrageenan/AAm solution was in liquid state, where loss modulus (G'') was greater than storage modulus (G'). As the temperature

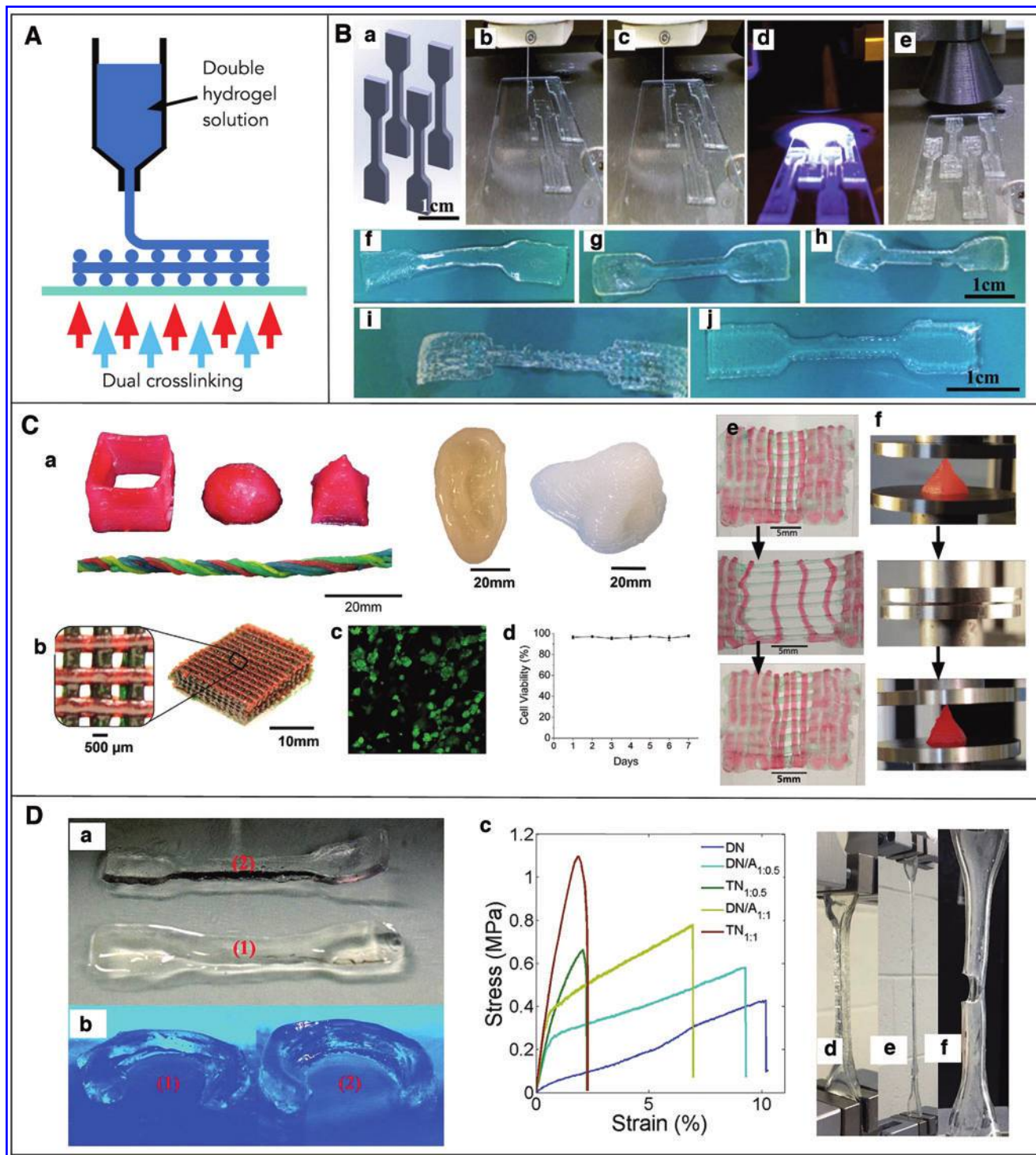


FIG. 5. (A) Schematic diagram of extrusion-based printing of DN gels structure. (B.a) Three dimensional computer-aided design of dog-bone structures. (B. b-e) Fabrication of dog-bones. (B.f-i) DN gel dog-bone structures printed by using alginate solution with concentrations of 2%, 3%, 4%, and 5% w/v at 25°C. (B.j) DN gel dog-bone structure printed using 5% w/v alginate solutions at 35°C.⁶³ (C) Printing of PEG/alginate hydrogel (C.a) different-shaped structures left. (C.b) Cell scaffold, which was used to host human embryonic kidney cells. (C.c) Live-dead imaging of HEK cell culture in the collagen-infused DN gels. (C.d) Cell viability plot derived from (C.e).⁶⁴ (D) Extrusion-based printing of agar/alginate/AAM gel (D.a) dog-bone-shaped structures using DN (1) and DN/A1:1 (2) (D.b) meniscus-shaped structures printed using DN 65°C and 45°C, (D.c) stress-strain plot for different concentrations of DN gels, (D.d) the tensile testing of the (D.e, D.f) DN/A1:1 hydrogel and TN1:1 gel. Here, DN:agar/PAAm double network hydrogel. DN/A:agar/PAAm double network hydrogel with uncrosslinked alginate. TN:agar/PAAm double network hydrogel with crosslinked alginate. The subscript, e.g. 1:1, represent weight ratio of agar to alginate.²⁵ Color images are available online.

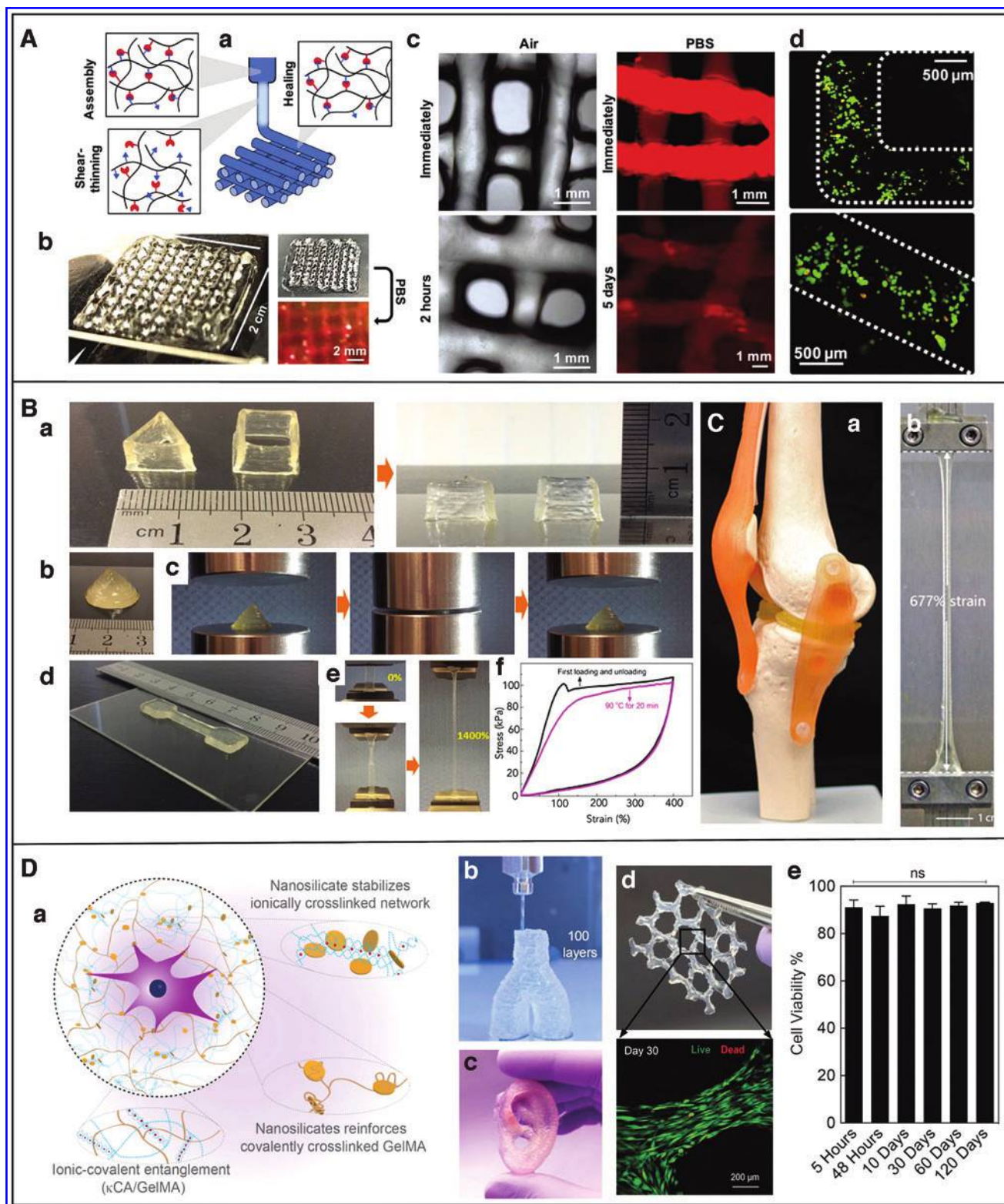


FIG. 6. (A) Extrusion-based 3D printing of DN gel structures functionalized HA. (A.a) Printing process of shear-thinning and self-healing of DN gels. (A.b) Image of 4-layer lattice structure in air and on immersion in PBS. (A.c) Zoomed view of images of lattices in air and on immersion in PBS (also stained with rhodamine-dextran). (A.d) Live–dead cell studies right after extrusion-based printing.²⁷ (B) Extrusion-based 3D printing of (AMPS)/AAM DN gel structures. (B.a) 3D-printed meniscus fitted in the knee model. (B.b) Dog-bone structure printed of (AMPS)/AAM DN after stretching to 677% strain.²⁶ (C) Extrusion-based 3D printing of κ -carrageenan/PAAm DN gels. (C.a) Triangle-shaped prism and cube structure and (C.b) cone structure (C.c) cone structure undergoing 90% compression and relaxation (C.d) printed dog-bone-shaped structure. (C.e) Stretching of the dog-bone structure with the strain of 14. (C.f) Stress–strain plot on first loading and unloading (black). Stress–strain plot showing the second loading and unloading after storing the sample at 90°C for 20 min after first loading and unloading.⁵³ (D) Extrusion-based printing of κ -carrageenan/GelMA hydrogel. (D.a) Schematic of nanoengineered ionic-covalent entanglement bioink. (D.b) Printing of structure with high aspect ratio (bifurcated vessel). (D.c) 3D printed ear. (D.d) 3D printing of encapsulated cells after 30 days in cell culture.⁶⁵ AMPS, 2-acrylamido-2-methylpropanesulfonate; GelMA, gelatin methacryloyl; HA, hyaluronic acid; PBS, phosphate buffered saline. Color images are available online.

started to decrease, there was a slight increase in G' and G'' . Further, decreasing the temperature close to a critical value increased the value of G' and G'' sharply, whereas at 44.7°C, G' surpasses G'' due to formation of a gel network. The gelation rate of the κ -carrageenan/AAM solution was high, which resulted in better three-dimension constructs. The authors claimed that this material system was better than the agar/AAM, which exhibited a larger gelation temperature range from 90°C to 30°C. This made it difficult to accurately control printing of constructs, when the agar/AAM solution was used for extrusion-based printing.

The κ -carrageenan/AAM material system was used to print several structures such as a mesh pattern, hollow triangular prism, hollow cube, and cube pattern. (Fig. 6C). The printed structures were compressed to 90% of the strain without significant deformation. These structures stretched 14 times their original length, and a necking behavior was observed during stretching. Further, self-healing behavior of the structures was demonstrated by gluing the broken structure together and storing them at temperature above sol-gel transition temperature. Above the transition temperature, carrageenan dissociated into a single chain, which, on cooling, re-associated into double helices, resulting in the self-healing of the structure. In addition, a strain sensor was fabricated by using these DN gels that correctly monitored and distinguished different motions of a human body.²⁶

Extrusion-based printers that cost merely \$300 have also been used to print DN gel structures. Wiley and colleagues used one of these inexpensive 3D printers to print structures of DN gels. In this work, the first network of the structure was printed by the extrusion-based printer using an ink that consisted of Laponite nanoclay, 2-acrylamido-2-methylpropanesulfonate (AMPS), crosslinker MBAA, and Irgacure 2959. Next, the structure was UV cured and soaked in a second network precursor made by dissolving AAM, MBAA, and Irgacure 2959 in water. After the structure was fully soaked, it was cured again in UV light. Laponite, a layered silicate nanoclay, provided a sufficient viscosity to facilitate extrusion of ink to print 3D structures.

Using this technique, they printed a pair of artificial menisci similar in shape and size to the human knee meniscus (Fig. 6B). The printed structures exactly fit a model joint without further modification. Several structures demonstrating the printing of high aspect ratio objects, overhangs, and complex anatomical features were printed, with the smallest feature size being 500 μm . Typically, calcium ions leach out of the DN gel structure on immersion in water. However, in this study, it was observed that the calcium ion did not leach out when soaked in deionized water. The tensile properties of the as-formed structures could be tweaked by varying the concentration of MBAA in the first network and the amount of AAM in the second network. They reported that the optimized structure showed an ultimate strain of around 900% and toughness of around 3000 kJ/m³ and the printed structure could be compressed to 80% strain without permanent deformation. The compression strength and stiffness of the optimized structures were observed to be higher than the bovine cartilage.⁵³

More recently, Gahawar and coworkers also used κ -carrageenan and reported nanoengineered ionic-covalent entanglement (NICE) bioink for extrusion-based 3D bioprinting. The bioink was prepared by using bioactive gelatin methacryloyl (GelMA), κ -carrageenan, and nanosilicates.

GelMA hydrogels are commonly used for cell culture, growth, and proliferation as they provide bio-environmental conditions similar to native extracellular matrix, including cell attachment sites. GelMA is thermally responsive, undergoes physical crosslinking at around 30°C, and stabilizes the structure during extrusion printing. Laponite XLG nanosilicates are disk-shaped mineral nanoparticles with a diameter of 30–50 nm and a thickness of 1 nm. The addition of nanosilicates increases the viscosity of DN gels, making them a better candidate for extrusion printing.

In this study, the performance of the NICE bioink was tested by using the I3 RepRap printer, which was loaded with bioink stored at 37°C, and structures were printed by using a 400 μm nozzle tip. Post-printing, the structures were photopolymerized with UV light and 5% KCl. Structures with different sizes and shapes such as a hollow cylinder with a shape like a human-scale bronchus or a Y-shaped bifurcated blood vessel were printed (Fig. 6D). The better printing capability of the bioink was attributed to physical gelation of GelMA in combination with the rheological effects of κ -carrageenan and nanosilicates. Further, incorporation of nanosilicate led to an improvement in adhesiveness and mechanical properties such as elasticity, viscoelastic modulus, and cell adhesion properties of the bioink. There was an increase in the strength and toughness of the reinforced DN gel structures compared with that of its parent gels. For instance, the compressive moduli doubled with each reinforcement mechanism. The improvement in the strength and toughness was due to stress sharing between networks and energy dissipation due to the ionic network breaking, whereas the covalent network remained intact. Later, the ionic network re-crosslinked on removal of stress.

Further, this reinforcement did not affect the water content and pore size, which makes the bioink an ideal candidate for bioprinting applications. Hence, the NICE bioink was mixed with cells and the cells were printed into 3D structures. The printed structures showed cell viability of more than 90% immediately after printing and throughout the 120-day period of cell culture. In addition, after a few days of the printing, the encapsulated cells proliferated and subsequently migrated toward the surface due to enhanced nutrition.⁶⁵

Extrusion-based printing was also used to print DN gels structures using natural hydrogels, namely HA and alginate. Inspired by mussel-adhesive chemistry, researchers modified catechol into HA that endowed adhesive properties. This modified HA formed a primary covalent network, whereas alginate enabled the ionic crosslinking-based secondary network that enhanced the mechanical properties of the primary covalent network. The as-formed material system is considered as a new promising material for bioprinting, as this method of fabrication using these gels was compatible with cell printing with improved cell viability.⁶⁶ Similarly, Hsieh and Hsu demonstrated the high-resolution biofabrication of DN gels structures using polyurethane (PU)-gelatin hydrogels. The printing technique is based on the ionic crosslinking of PU and thermal crosslinking of gelatin. Several structures such as cell scaffolds, nose-shaped structures were printed by using an 80 μm nozzle and these structures showed excellent compression properties. This printing strategy exhibited several advantages such as biocompatibility, a simple and convenient printing process, high stacking ability, and a resolution better than 100 μm .⁶⁷

Similar to extrusion-based printing, inkjet printing has been also used to fabricate 3D structure by using DN gels. Inkjet printing is a mask-free, high-resolution rapid printing technology where inks are deposited by multiple printheads to print 2D/3D structures. On this note, Stringer and colleagues demonstrated inkjet printing of poly(3,4-ethylene-dioxythiophene):poly(styrenesulfonate) (PEDOT:PSS) hydrogel by in-air coalescence of PEDOT:PSS and ionic liquid (IL), where droplets of the PEDOT:PSS/IL hydrogel of size $\approx 260 \mu\text{m}$ were fabricated within $\approx 600 \mu\text{s}$ and deposited to print structures. This technique was demonstrated to pattern electrodes and print structures such as microfluidic devices. This strategy of printing exhibits high potential for many applications, especially in the field of flexible electronics.⁶⁸

Optics-Based Printing of DN Gels

Various optics-based fabrication methods such as OPL, two-photon polymerization, stereolithography (SLA), and hybrid laser printing have been used to print high-resolution structures for a wide range of applications.^{54,69–76} In these methods, light is used to crosslink or polymerize a liquid photosensitive resin or prepolymer solution into 2D/3D solid structures. Only recently, these methods have been used to print DN gels into 2D and 3D user-defined structures.

One lithography technique that is being widely used in the biomedical engineering field is OPL.^{54,69} In this method, light patterns are generated by using digital mask generators such as digital micromirror devices (DMD), liquid crystal-based spatial light modulators, or light-based projectors (Fig. 7A).^{54,69,77} OPL-based printing was used by Alsberg and coworkers to demonstrate the patterning of simple 2D structures of DN alginate. They employed alginate with a methacrylate functional group that could undergo both ionic and covalent crosslinking. As mentioned earlier, alginate undergoes ionic crosslinking when it comes in contact with divalent ion such as calcium, whereas UV light covalently crosslinks alginate due to the presence of the methacrylate groups. Local regulations due to different crosslinking mechanisms were used as guidance cues for cellular alignment. (Fig. 7B).⁷⁸

Ge and colleagues reported optical 3D printing of covalent DN gel structures, which can stretch more than 13 times their original length. In this work, the prepolymer solution consisted of 50–80% water, AAm, PEGDA, and highly efficient photoinitiator 2,4,6-trimethylbenzoyl-diphenylphosphine oxide (TPO) nanoparticles. Here, AAm was used for stretchability, whereas PEGDA was used to adjust the crosslinking density and modulate the mechanical properties. They modified TPO (commercial photoinitiator, typically available in powder form) into highly water-soluble TPO nanoparticles; this increased its crosslinking efficiency to 9 times that of the commonly used Irgacure 2959 photoinitiator. The DMD-modulated light was used to crosslink layers of prepolymer solution by rendering double bonds on acrylamide and PEGDA, resulting in a 3D structure that exhibited a strain of 1300%. Printed structures were shown to be biocompatible with cell viabilities of 93% with fibroblast cells and liver cancer cells, respectively.

Multimaterial printing of hydrogel–elastomer hybrids, printed by the above mentioned method, exhibited strong interfacial bonding. This was attributed to the presence of

covalent bonds between the hydrogel and the elastomer. Lastly, lithium chloride was added to the hydrogel solution and an electrical circuit was printed that maintained electrical conductivity even after being subjected to large deformations (Fig. 7C). The printed structures were highly transparent at a visible spectrum of light, and the transmittance dropped in the UV region as the TPO nanoparticles absorbed the UV light drastically. This makes the hydrogel ideal material for printing optical components such as lens.⁵¹

Soman and coworkers also used OPL to print 2D and 3D structures by using a DN gel in a two-step crosslinking process that involved photo-crosslinking of the desired structure using UV light followed by immersion of the printed structure into a divalent ion bath to enable ionic crosslinking. The hydrogel prepolymer solution consisted of PAAm, alginate, MBAAm (crosslinker), and LAP photoinitiator in water (80% v/v). Similar to previous studies, the mechanical performance of printed DN gel structures was better in terms of strain and toughness as compared with its individual parent gels. They also reported that the light dose has a significant effect on the tensile properties of DN gel structures. The partially exposed sample and overexposed sample exhibited lower strain values compared with the structures that received the minimum light dose, which crosslinked the structure just enough to retain its shape. User-defined 2D patterns such as “Syracuse University” and re-entrant honeycomb “auxetic” geometry, and 3D structures such as “The Empire State Building” and a “Mayan pyramid” were printed at high resolution (Fig. 7D).⁵⁴

A comparative table is provided next to summarize the 2D/3D printing of the different DN gels’ structures (Table 1).

Challenges, Future Outlook, and Concluding Remarks

The DN hydrogels possess extraordinary mechanical properties, and have attracted great attention in recent years, with applications ranging from tissue engineering to flexible electronics. Although the synthesis of DN hydrogels was first reported almost a decade and a half ago, the 3D printing of DN gels is still in its infancy and several challenges exist. At present, the printing of DN gels is mostly limited to a few fabrication techniques and material compositions; this must be solved before DN gels can be widely adopted by the research community. With current methods, multiscale 3D structures using DN gels that incorporate undercuts, overhangs, and channels are difficult to print. This would require balancing the aspects of printability while maintaining the unique mechanical properties of DN gels.

For extrusion-based printing, choosing a DN composition that exhibits the necessary viscosity and crosslinking mechanics is the key, whereas for optics-based printing, understanding the photo-crosslinking process become important. At present, conventional molding/casting and extrusion-based 3D printing methods of fabricating DN structures provide a printing resolution of hundreds of micrometers. Although optics-based fabrication methods have the potential to print complex 3D structures using DN gels at microscale resolution, key issues with printing dual ionic-covalent networks need to be solved. A better understanding of DN gels from the materials perspective (use of other polymers and/or functional groups) and the exploration of other optical

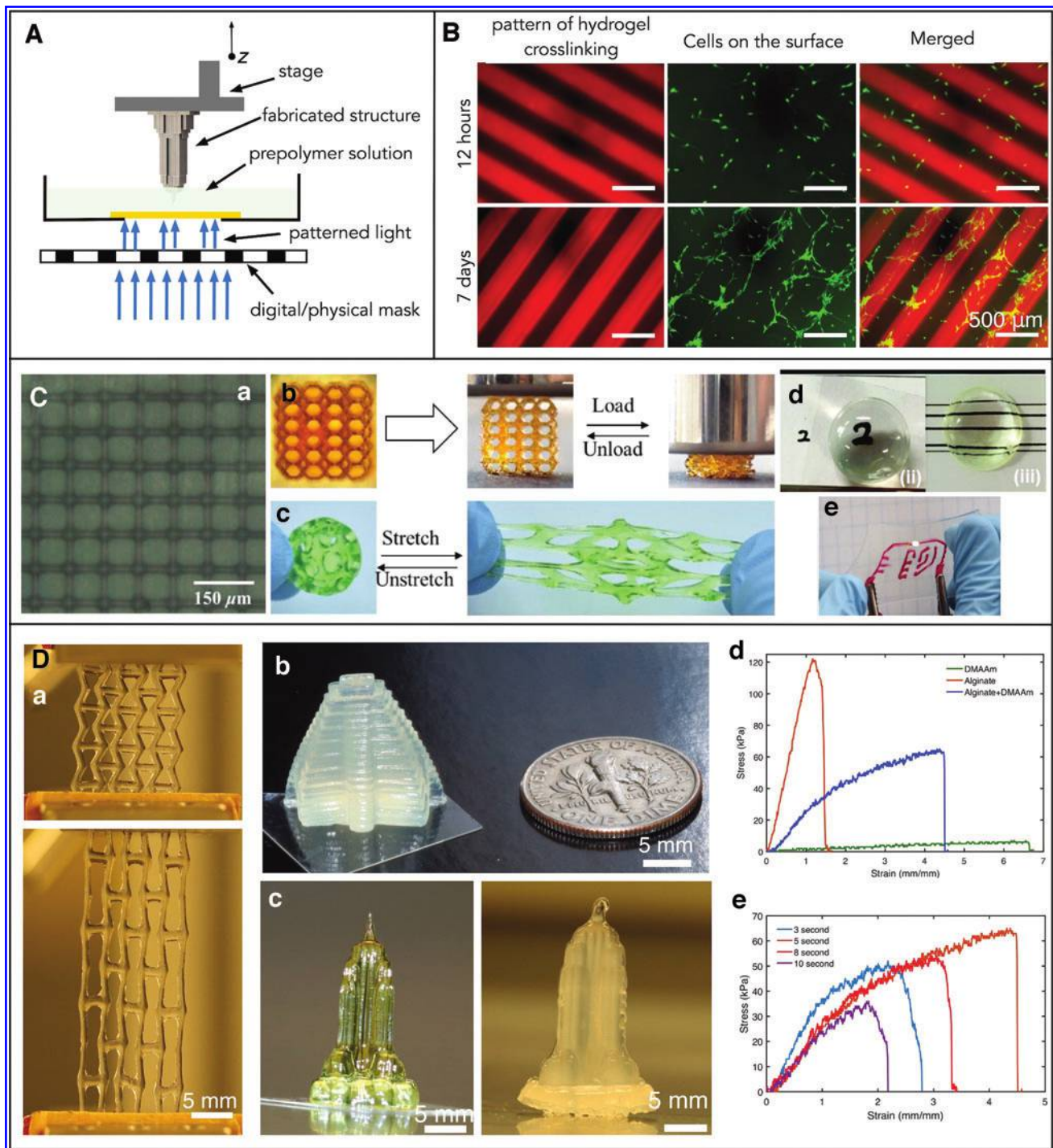


FIG. 7. Optics-based 3D printing of DN gels. (A) Schematic of 2D/3D printing using optical projection lithography. (B) Optical patterning of methacrylated alginate gels. Fluorescence image of alginate DN gels and cells recorded after 12 h (top row), and after 7 days in culture (bottom row).⁷⁸ (C) Optics-based fabrication of 3D structure using acrylamide-PEGDA DN gels. (C.a) 3D printed grid with resolution of $7\ \mu\text{m}$. (C.b, C.c) Stretchable and compressible 3D printed DN gels structures, (C.d) soft lens printed using DN gels, (C.e) demonstration of stretchable electronics using printed DN gels.⁵¹ (D) Optics-based printing of Alginate/PMAA DN gels. (D.a) Printing of auxetic shape 2D structure. (D.b, D.c) Printing of 3D structure such as Mayan pyramid and Empire state building (images after photocrosslinking, left, and after subsequent ionic crosslinking, right). (D.d) Stress-strain curve of the DN gel structure, AAm hydrogel structure, and alginate hydrogel structure. (D.e) Stress-strain plot obtained from the printed DN gel structures exposed to various exposure times.⁵⁴ 2D, two-dimensional; PEGDA, poly(ethylene glycol) diacrylate. Color images are available online.

TABLE 1. SUMMARY OF THREE-DIMENSIONAL PRINTING OF DOUBLE-NETWORK HYDROGELS: COMPARISON OF THREE-DIMENSIONAL PRINTED STRUCTURES IN TERMS OF PRINTING TECHNIQUES, RESOLUTION OF PRINTING, WATER CONTENT, AND TENSILE PROPERTIES

Printing techniques	Materials	Resolution of printing	Water content (%)	Maximum tensile stress (MPa)	Elastics modulus (MPa)	Ultimate strain (%)	References
Casting and molding-based printing	Cartilage	—	70–85	35.7	0.45–0.80	—	19
	PAMPS/PVA	Low	90	—	0.15	~300	55
	PAMPS/AAm	Low	>90	—	—	—	56
	Alginate/PAAm	Low	~90	0.17	0.066	2000	28
	Agar/PAAm	Low	~80	~1	—	2000	58
	PEG/agarose	Low	>90	—	—	—	44
Extrusion-based printing	PVA/AAm	Low	~90	~0.19	~0.080	500	59
	Alginate/AAm	~0.3 mm	80	0.20	~0.07	300	63
	Alginate/PEGDA	0.5 mm	~78	—	—	600	64
	Agar/alginate/PAAm	0.4 mm	~75	1.096	0.87	~230	25
	Nor-HA/HA-HYD/ HA-ALD	0.36 mm	—	—	—	—	27
	κ -carrageenan/AAm	0.30 mm	~80	0.7	0.35	1400	26
Optics-based printing	AMPS/AAm	0.50 mm	~80	~1.4	~1	~900	53
	κ -carrageenan/GelMA	0.40 mm	~85	~0.18	~0.5	~30	65
	Methacrylated alginate/ alginate	<0.100 mm	—	—	—	—	78
	PEGDA/AAm	0.007 mm	50–80	~0.025	0.05–0.250	500–1300	51
	Alginate/AAm	0.100 mm	80%	0.1	0.06	450	54

AAm, acrylamide; AMPS, 2-acrylamido-2-methylpropanesulfonate; GelMA, gelatin methacryloyl; HA-ALD, hyaluronic acid-aldehyde; HA-HYD, hyaluronic acid-hydrazide; Nor-HA, norbornenes-hyaluronic acid; PAAm, polyacrylamide; PAMPS, poly(2-acrylamide-2-methylpropane sulfonic acid); PEG, polyethylene glycol; PEGDA, poly(ethylene glycol) diacrylate; PVA, polyvinyl alcohol.

printing methods (direct laser writing, micro-SLA) has the potential to make DN-3D structures with a higher degree of complexity and improved resolution.

Reports of 3D printing DN gels are mostly concentrated to PAAm gel. Consideration of the new hydrogel materials that are similar to the PAAm network will lead to 3D structures of DN gels with new functionalities and applications. Although many DN gels have been shown to be compatible with cell culture, printing of the cell-laden DN gels into customized 3D shapes could open up new application areas in tissue engineering. Only a handful of groups are able to print these structures using extrusion-based printing, which does not provide sufficient resolution and shape fidelity. A possible solution for printing complicated geometries would be a combination of techniques such as a hybrid laser printer, which allows for the printing of hydrogel structures in both additive (crosslinking) and subtractive (ablation) manner. Special focus should be placed on natural and degradable hydrogels as well as self-healing biomaterials, which will greatly benefit the field of tissue engineering.

Currently, printing of self-healing DN gels is limited only to simple structures; printing user-defined 3D structures that can self-heal has high potential in tissue engineering. Further, incorporation of novel optical, electric, and magnetic nanoparticles during the printing process can potentially realize a range of new functional materials. In addition, new DN gels with shape-changing or deformation properties would benefit the field of soft robotics. Although it is well known that the mechanical strength of DN gels depends on how the network fractures and how energy is dissipated, an in-depth mechanistic understanding of the contributions of intra- and inter-network interactions, heterogeneity within networks, and distribution of fractures within the network is needed to

rationally synthesize new DN gels. Further, current understanding about toughening, necking, yielding, and softening recovery behavior within DN gels is not complete. A comprehensive theoretical study combined with computational modeling and simulation is also required to discover new structure–property–application relationships that will guide the 3D printing of DN gels in the coming decades.

Authors' Contributions

P.K. and P.S. wrote the article.

Acknowledgment

The authors would like to thank Dr. Ameya Narkar for proofreading and key insightful comments.

Author Disclosure Statement

The authors declare no conflict of interest.

Funding Information

This work was partially supported by NIH R21GM129607 and R21AR076645 awarded to Prof. Pranav Soman.

References

- Li J, Mooney DJ. Designing hydrogels for controlled drug delivery. *Nat Rev Mater* 2016;1:16071.
- Zhang YS, Khademhosseini A. Advances in engineering hydrogels. *Science* (80-) 2017;356:1–10. DOI: 10.1126/science.aaf3627.

3. Howard D, Buttery LD, Shakesheff KM, *et al.* Tissue engineering: strategies, stem cells and scaffolds. *J Anat* 2008;213:66–72.
4. Ahmed EM. Hydrogel: preparation, characterization, and applications: a review. *J Adv Res* 2015;6:105–121.
5. Mahinroosta M, Jomeh Farsangi Z, Allahverdi A, *et al.* Hydrogels as intelligent materials: a brief review of synthesis, properties and applications. *Mater Today Chem* 2018;8:42–55.
6. Maitra J, Shukla VK. Cross-linking in hydrogels—a review. *Am J Polym Sci* 2014;4:25–31.
7. Oyen ML. Mechanical characterisation of hydrogel materials. *Int Mater Rev* 2014;59:44–59.
8. Billiet T, Vandenhaute M, Schelfhout J, *et al.* A review of trends and limitations in hydrogel-rapid prototyping for tissue engineering. *Biomaterials* 2012;33:6020–6041.
9. Zheng J. Fundamentals of double network hydrogels. *J Mater Chem B* 2015;3:3654–3676.
10. Gong JP. Why are double network hydrogels so tough? *Soft Matter* 2010;6:2583–2590.
11. Rafeian S, Mirzadeh H, Mahdavi H, *et al.* A review on nanocomposite hydrogels and their biomedical applications. *IEEE J Sel Top Quantum Electron* 2019;26:154–174.
12. Jiang L, Liu C, Mayumi K, *et al.* Highly stretchable and instantly recoverable slide-ring gels consisting of enzymatically synthesized polyrotaxane with low host coverage. *Chem Mater* 2018;30:5013–5019.
13. Jiang F, Huang T, He C, *et al.* Interactions affecting the mechanical properties of macromolecular microsphere composite hydrogels. *J Phys Chem B* 2013;117:13679–13687.
14. Zhang HJ, Luo F, Ye Y, *et al.* Tough triblock copolymer hydrogels with different micromorphologies for medical and sensory materials. *ACS Appl Polym Mater* 2019;1:1948–1953.
15. Fujii K, Asai H, Ueki T, *et al.* High-performance ion gel with tetra-PEG network. *Soft Matter* 2012;8:1756–1759.
16. Nonoyama T, Gong JP. Double-network hydrogel and its potential biomedical application: a review. *Proc Inst Mech Eng Part H J Eng Med* 2015;229:853–863.
17. Liang Z, Liu C, Li L, *et al.* Double-network hydrogel with tunable mechanical performance and biocompatibility for the fabrication of stem cells- encapsulated fibers and 3D assemble. *Sci Rep* 2016;6:33462.
18. Gu Z, Huang K, Luo Y, *et al.* Double network hydrogel for tissue engineering. *Wiley Interdiscip Rev Nanomedicine Nanobiotechnology* 2018;10:1–15.
19. Yongmei C, Kun D, Zhenqi LIU, *et al.* Double network hydrogel with high mechanical strength: performance, progress and future perspective. *Technol Sci* 2012;55:2241–2254.
20. Gong JP, Katsuyama Y, Kurokawa T, *et al.* Double-network hydrogels with extremely high mechanical strength. *Adv Mater* 2003;15:1155–1158.
21. Nakajima T, Sato H, Zhao Y, *et al.* A universal molecular stent method to toughen any hydrogels based on double network concept. *Adv Funct Mater* 2012;22:4426–4432.
22. Liu XJ, Ren XY, Guan S, *et al.* Highly stretchable and tough double network hydrogels via molecular stent. *Eur Polym J* 2015;73:149–161.
23. Lin T, Shi M, Huang F, *et al.* One-pot synthesis of a double-network hydrogel electrolyte with extraordinarily excellent mechanical properties for a highly compressible and bendable flexible supercapacitor. *ACS Appl Mater Interfaces* 2018;10:29684–29693.
24. Chen P, Wu R, Wang J, *et al.* One-pot preparation of ultrastrong double network hydrogels. *J Polym Res* 2012;19:1–4. DOI: 10.1007/s10965-012-9825-5.
25. Wei J, Wang J, Su S, *et al.* 3D printing of an extremely tough hydrogel. *RSC Adv* 2015;5:81324–81329.
26. Liu S, Li L. Ultrastretchable and self-healing double-network hydrogel for 3D printing and strain sensor. *ACS Appl Mater Interfaces* 2017;9:26429–26437.
27. Wang LL, Highley CB, Yeh Y, *et al.* Three-dimensional extrusion bioprinting of single- and double-network hydrogels containing dynamic covalent crosslinks. *J Biomed Mater Res Part A* 2018;106A:865–875.
28. Sun J, Zhao X, Illeperuma WRK, *et al.* Highly stretchable and tough hydrogels. *Nature* 2012;489:133–136.
29. Darnell MC, Sun J, Mehta M, *et al.* Biomaterials performance and biocompatibility of extremely tough alginate/polyacrylamide hydrogels. *Biomaterials* 2013;34:8042–8048.
30. Deng Y, Huang M, Sun D, *et al.* Dual physically cross-linked κ -carrageenan-based double network hydrogels with superior self-healing performance for biomedical application. *ACS Appl Mater Interfaces* 2018;10:37544–37554.
31. Wu F, Chen L, Wang Y, *et al.* Tough and stretchy double-network hydrogels based on in situ interpenetration of polyacrylamide and physically cross-linked polyurethane. *J Mater Sci* 2019;54:12131–12144.
32. Dekosky BJ, Dormer NH, Ingavle GC, *et al.* Hierarchically designed agarose and poly(ethylene glycol) interpenetrating network hydrogels for cartilage tissue engineering. *Tissue Eng Part C Methods* 2010;16:1533–1542.
33. Li J, Suo Z, Vlassak JJ. Stiff, strong, and tough hydrogels with good chemical stability. *J Mater Chem B* 2014;2:6708–6713.
34. Wei D, Yang J, Zhu L, *et al.* Fully physical double network hydrogels with high strength, rapid self-recovery and self-healing performances. *Polym Test* 2018;69:167–174.
35. Chen Q, Wei D, Chen H, *et al.* Simultaneous enhancement of stiffness and toughness in hybrid double-network hydrogels via the first, physically linked network. *Macromolecules* 2015;48:8003–8010.
36. Lin T, Shi M, Huang F, *et al.* One-pot synthesis of a double-network hydrogel electrolyte with extraordinarily excellent mechanical properties for a highly compressible and bendable flexible supercapacitor. *ACS Appl Mater Interfaces* 2018;10:29684–29693.
37. Balakrishnan B, Joshi N, Jayakrishnan A, *et al.* Self-crosslinked oxidized alginate/gelatin hydrogel as injectable, adhesive biomimetic scaffolds for cartilage regeneration. *Acta Mater* 2014;10:3650–3663. DOI: 10.1016/j.actbio.2014.04.031.
38. Rennerfeldt DA, Renth AN, Talata Z, *et al.* Tuning mechanical performance of poly (ethylene glycol) and agarose interpenetrating network hydrogels for cartilage tissue engineering. *Biomaterials* 2013;34:8241–8257.
39. Weng L, Gouldstone A, Wu Y, *et al.* Mechanically strong double network photocrosslinked hydrogels from N, N-dimethylacrylamide and glycidyl methacrylated hyaluronan. *Biomaterials* 2008;29:2153–2163.

40. Ingavle GC, Dormer NH, Gehrke SH, *et al.* Using chondroitin sulfate to improve the viability and biosynthesis of chondrocytes encapsulated in interpenetrating network (IPN) hydrogels of agarose and poly(ethylene glycol) diacrylate. *J Mater Sci Mater Med* 2012;23:157–170.
41. Liao IC, Moutos FT, Estes BT, *et al.* Composite three-dimensional woven scaffolds with interpenetrating network hydrogels to create functional synthetic articular cartilage. *Adv Funct Mater* 2013;23:5833–5839.
42. Yasuda K, Kitamura N, Gong JP, *et al.* A novel double-network hydrogel induces spontaneous articular cartilage regeneration in vivo in a large osteochondral defect. *Macromol Biosci* 2009;9:307–316.
43. Yoshikawa K, Kitamura N, Kurokawa T, *et al.* Hyaluronic acid enhances in vitro induction effects of synthetic PAMPS and PDMAAm hydrogels on chondrogenic differentiation of ATDC5 cells. *Arthrosc J Arthrosc Relat Surg* 2013;29:e134–e135.
44. Bu Y, Shen H, Yang F, *et al.* Construction of tough, in situ forming double-network hydrogels with good biocompatibility. *ACS Appl Mater Interfaces* 2017;9:2205–2212.
45. Zhao Y, Nakajima T, Yang JJ, *et al.* Proteoglycans and glycosaminoglycans improve toughness of biocompatible double network hydrogels. *Adv Mater* 2014;26:436–442.
46. Bae KH, Wang LS, Kurisawa M. Injectable biodegradable hydrogels: progress and challenges. *J Mater Chem B* 2013;1:5371–5388.
47. Pacelli S, Paolicelli P, Pepi F, *et al.* Gellan gum and polyethylene glycol dimethacrylate double network hydrogels with improved mechanical properties. *J Polym Res* 2014;21:409.
48. Murosaki T, Ahmed N, Ping Gong J. Antifouling properties of hydrogels. *Sci Technol Adv Mater* 2011;12:064706.
49. Ajiro H, Watanabe J, Akashi M. Cell adhesion and proliferation on poly(N-vinylacetamide) hydrogels and double network approaches for changing cellular affinities. *Biomacromolecules* 2008;9:426–430.
50. Bakarich SE, Gorkin R, Panhuis MIH, *et al.* 4D printing with mechanically robust, thermally actuating hydrogels. *Macromol Rapid Commun* 2015;36:1211–1217.
51. Zhang B, Li S, Hingorani H, *et al.* Highly stretchable hydrogels for UV curing based high-resolution multimaterial 3D printing. *J Mater Chem B* 2018;6:3246–3253.
52. Chan HN, Shu Y, Tian Q, *et al.* Replicating 3D printed structures into hydrogels. *Mater Horizons* 2016;3:309–313.
53. Yang F, Tadepalli V, Wiley BJ. 3D printing of a double network hydrogel with a compression strength and elastic modulus greater than those of cartilage. *ACS Biomater Sci Eng* 2017;3:863–869.
54. Kunwar P, Jannini AVS, Xiong Z, *et al.* High-resolution 3D printing of stretchable hydrogel structures using optical projection lithography. *ACS Appl Mater Interfaces* 2020;12:1640–1649.
55. Nakajima T, Takedomi N, Kurokawa T, *et al.* A facile method for synthesizing free-shaped and tough double network hydrogels using physically crosslinked poly(vinyl alcohol) as an internal mold. *Polym Chem* 2010;1:693–697.
56. Saito J, Furukawa H, Kurokawa T, *et al.* Robust bonding and one-step facile synthesis of tough hydrogels with desirable shape by virtue of the double network structure. *Polym Chem* 2011;2:575–580.
57. Li Y, Wang C, Zhang W, *et al.* Preparation and characterization of PAM/SA tough hydrogels reinforced by IPN technique based on covalent/ionic crosslinking. *J Appl Polym Sci* 2015;132:1–7.
58. Chen Q, Zhu L, Zhao C, *et al.* A robust, one-pot synthesis of highly mechanical and recoverable double network hydrogels using thermoreversible sol-gel polysaccharide. *Adv Mater* 2013;25:4171–4176.
59. Ge G, Zhang Y, Shao J, *et al.* Stretchable, transparent, and self-patterned hydrogel-based pressure sensor for human motions detection. *Adv Funct Mater* 2018;28:1–8.
60. Ning L, Chen X. A brief review of extrusion-based tissue scaffold bio-printing. *Biotechnol J* 2017;12:1–16. DOI: 10.1002/biot.201600671.
61. Ozbolat IT, Hospodiuk M. Current advances and future perspectives in extrusion-based bioprinting. *Biomaterials* 2016;76:321–343.
62. Naghieh S, Sarker M, Izadifar M, *et al.* Dispensing-based bioprinting of mechanically-functional hybrid scaffolds with vessel-like channels for tissue engineering applications—a brief review. *J Mech Behav Biomed Mater* 2018;78:298–314.
63. Bakarich SE, Beirne S, Wallace G, *et al.* Extrusion printing of ionic-covalent entanglement hydrogels with high toughness. *J Mater Chem B* 2013;1:4939–4946.
64. Hong S, Sycks D, Chan HF, *et al.* 3D printing of highly stretchable and tough hydrogels into complex, cellularized structures. *Adv Mater* 2015;27:4035–4040.
65. Chimene D, Peak CW, Gentry JL, *et al.* Nanoengineered ionic-covalent entanglement (NICE) bioinks for 3D bioprinting. *ACS Appl Mater Interfaces* 2018;10:9957–9968.
66. Guo Z, Xia J, Mi S, *et al.* Mussel-inspired naturally derived double-network hydrogels and their application in 3D printing: from soft, injectable bioadhesives to mechanically strong hydrogels. *ACS Biomater Sci Eng* 2020;6:1798–1808.
67. Hsieh CT, Hsu SH. Double-network polyurethane-gelatin hydrogel with tunable modulus for high-resolution 3D bioprinting. *ACS Appl Mater Interfaces* 2019;11:32746–32757.
68. Teo MY, Ravichandran N, Kim N, *et al.* Direct patterning of highly conductive PEDOT:PSS/ionic liquid hydrogel via microreactive inkjet printing. *ACS Appl Mater Interfaces* 2019;11:37069–37076.
69. Tumbleston JR, Shirvanyants D, Ermoshkin N, *et al.* Continuous liquid interface production of 3D objects. *Science* (80-) 2015;347:1349–1352.
70. Kunwar P, Hassinen J, Bautista G, *et al.* Direct laser writing of photostable fluorescent silver nanoclusters in polymer films. *ACS Nano* 2014;8:11165–11171.
71. Sun HB, Kawata S. Two-photon photopolymerization and 3D lithographic microfabrication. *Adv Polym Sci* 2004;170:169–273.
72. Xiong Z, Liu H, Tan X, *et al.* Diffraction analysis of digital micromirror device in maskless photolithography system. *J Micro Nanolithogr MEMS MOEMS* 2014;13:043016.
73. Kunwar P, Turquet L, Hassinen J, *et al.* Holographic patterning of fluorescent microstructures comprising silver nanoclusters. *Opt Mater Express* 2016;6:697–698.

74. Kunwar P, Hassinen J, Bautista G, *et al.* Sub-micron scale patterning of fluorescent silver nanoclusters using low-power laser. *Sci Rep* 2016;6:6–11.
75. Xiong Z, Li H, Kunwar P, *et al.* Femtosecond laser induced densification within cell-laden hydrogels results in cellular alignment. *Biofabrication* 2019;11:1–11. DOI: 10.1088/1758-5090/ab0f8b.
76. Kunwar P, Xiong Z, Mcloughlin ST, *et al.* Oxygen-permeable films for continuous additive, subtractive, and hybrid additive/subtractive manufacturing. *3D Print Addit Manuf* 2020;7:216–221.
77. Grigoryan B, Paulsen SJ, Corbett DC, *et al.* Multivascular networks and functional intravascular topologies within biocompatible hydrogels. *Science* (80-) 2019;364:458–464.
78. Samorezov JE, Morlock CM, Alsberg E. Dual ionic and photo-crosslinked alginate hydrogels for micropatterned spatial control of material properties and cell behavior. *Bioconjug Chem* 2015;26:1339–1347.

Address correspondence to:

Pranav Soman
Department of Chemical and Bioengineering
Syracuse University
Syracuse, NY
USA

E-mail: psoman@syr.edu